Carpathian Journal of Earth and Environmental Sciences, November 2013, Vol. 8, No. 4, p. 27 - 33

3D MODELLING AND STRUCTURAL INVESTIGATION OF THE CENTRAL VOLCANICS IN SLOVAKIA USING MAGNETIC DATA

Özcan BEKTAŞ[1*], Aydın BÜYÜKSARAÇ[2] & Kamil ROZIMANT[3]

[1]Cumhuriyet University, Faculty of Engineering, Department of Geophysical Engineering, Sivas TR-58140, Turkey, Phone: +90-346-2191010 Ext:1925, Fax: +90-346-2191190, e-mail: obektas@cumhuriyet.edu.tr

[2]Çanakkale Onsekiz Mart University, Faculty of Engineering and Architecture, Department of Geophysical Engineering, Çanakkale TR-17020, Turkey, e-mail: absarac@comu.edu.tr

[3]Comenius University, Faculty of Natural Sciences,Department of Applied and Environmental Geophysics, Bratislava, Slovakia, e-mail: rozimant@fns.uniba.sk

Abstract: The Central volcanics, located in central part of Slovakia, is characterized by intense andesitic volcanic activity that resulted in the formation of stratavolcanoes and dome complexes of Middle and Late Miocene age. The basement area has been affected tectonically resulting in the formation of horst and graben structures. The Central Slovakian Volcanic Field (CSVF) exhibits a very complex magnetic anomaly. A 3-km upward continued magnetic map indicates a deep-seated source for this magmatism. The pseudogravity transformation of the upward continued anomaly has also been constructed. This anomaly was modelled by a 3D-method. The anomalous body lies between the depths of 4.4 to 8.5 km beneath the surface of the CSVF. Volcanic structures and some lineaments are presented on the maxima of the horizontal gradient of the pseudogravity anomaly map. They are well correlated with the structural map of CSVF.

Key Words: magnetic anomalies**;** 3D magnetic model; Central Slovakian Volcanic Field; power spectrum; maxima of horizontal gradient

1. INTRODUCTION

The thick Tertiary sedimentary and volcanic rock complexes related to the Pannonian back-arc basin system cover a large part of the central and most of the inner part of the Western Carpathians (Zeyen et al., 2002). The topography in the central part of Slovakia is very rugged because of the presence of several mountain ranges. The tectonic processes and the geological composition have substantially affected the geomorphology of the mountain massifs in this region. The mountain ranges in the Carpathians can be distinguished into three different arc-shaped zones. The first zone comprises of a flysh belt along the northern margin of the Carpathians; the second zone comprises of a group of central core mountain ranges in the middle; and finally, the last zone comprises of several volcanic ranges on the southern periphery of the Carpathians. Slovakia has two distinct geological and geomorphological formations: the Carpathian Arc and its adjacent lowland areas. These two formations were collectively shaped by young tectonics, Tertiary volcanism, glacial sculpturing and fluvial processes (Plašienka et al., 1997; Bielik et al., 2004).

Volcanic mountain ranges in Slovakia are predominantly stratavolcanic. The younger volcanic basalts originated from the lava flows along the river valleys. These basaltic flows often form rocky peaks and elevated ridges. The less resistant pyroclastic rock formations such as tuffs and tuffites usually represent the smoother parts, while the massive andesites and basalts represent the steeper to rocky parts of the mountain slopes. Figure 1 shows the Central Slovakian Volcanic Field (CSVF) in a scheme of the geological map of Slovakia. Rozimant et al., (2009) calculated the Curie Point Depth of Slovakia and found that its shallowest depth occurs beneath the Central Volcanics (around 15–17 km depth). Very high heat flow values were also recorded in this region (90–100 mWm^{-2}).

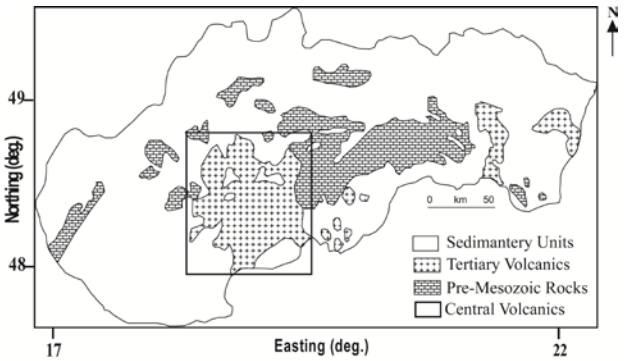

Figure 1. A simplified geological map of Slovakia (after Túnyi & Márton, 2002).

The western Carpathian gravity low zone extends over territories of the northern and part of the central Slovakia. The Western Carpathian gravity low zone consists of two parts: the Outer Western Carpathian gravity low and the Inner Western Carpathian gravity low. The positive gravity anomaly caused by the Moho elevation and by the high density upper and lower crustal anomalies collectively superimpose over the negative gravity anomaly caused by the asthenosphere. The upper and lower crustal anomalies are mainly caused by the core mountains, pre-Tertiary basement elevations, basaltic volcanism and presence of dense metamorphic and basic rocks in the crust. The latter stage of the development of the Western Carpathian Arc and the Pannonian Basin were characterized by a lithospheric disintegration that occurred as a consequence of the transition from a transpressional to an extensional regime. This process was accompanied by crustal thinning as well as lithospheric thinning. The thinning of the lithosphere was accompanied by uplifting of the partially molten masses from the asthenosphere, rich in asthenoliths (Šefara et al., 1996).

The southern part of Slovak gravity high is divided into three parts: (1) the western part where positive anomalies have resulted from the elevation of the pre-Tertiary basement; (2) the central part where the youngest basaltic volcanism is observed; and (3) the eastern part where Palaeozoic metamorphites and core mountains are present. In this region, local negative anomalies can also be observed, mainly because of the low-density graben sedimentary fills and the granitic rocks. Some local negative gravity anomalies are also caused by the geology of the Central volcanic region (Bielik et al., 2006).

The Central volcanics present a very different structure in the Western Carpathian. However, investigation of the Central volcanics is very important for understanding the source of the volcanoes and the effect of tectonics on them. Magnetic anomalies can be also used to differentiate between different volcanic units.

2. GEOLOGICAL AND TECTONIC SETTINGS

The Western Carpathians are composed of tectonically active mountain ranges. The tectonic processes and the geological composition have greatly affected the geomorphology of this region.

The CSVF have a horst and graben-like structure. The evolutionary phase of the CSVF have been dated between the Middle and Late Miocene time (16.5–6 Ma); this phase was accompanied by an extensive, dominantly andesitic volcanic activity, giving rise to a number of stratavolcanoes and dome/flow complexes. The salient geological features of this system are as follows: **(a)** the dominant N–S trending horst and grabens in the central part; **(b)** the NE–SW trending horsts and grabens; **(c)** the NW–SE trending structural elements; **(d)** volcano-tectonic features such as Kremnica graben, Štiavnica caldera and resurgent horst, Javorie graben, and Pol'ana depression; and **(e)** a frequent occurrence of asymmetric horst and grabens, including the half-graben structure (Konečný & Lexa, 2002).

Konečný & Lexa (2002) described the evolution of the horst and graben structure and the related volcanism in the CSVF in seven following stages:
(i) The Early Badenian evolution of the area was followed by the Early Miocene denudation and levelling. The individual volcanic centres were situated especially along the marginal faults of the grabens and along the N–S striking faults. **(ii)** Andesite volcanic activity during the late Early to early Late Badenian was responsible for the formation of two monogene volcanoes and several extensive stratavolcanoes. **(iii)** During the Late Badenian, the subsidence of the Upper Nitra depression at the NE edge of the region continued resulting in the formation of the Handlova and Novaky coal-basin. The extensive stratavolcanoes in other parts of the region passed through the stage of the caldera or volcano-tectonic graben formation. **(iv)**The evolution of the stratavolcanoes continued throughout the Early-Middle Sarmatian time, erupting mostly the undifferentiated pyroxene and pyroxene-amphibole andesites. **(v)** The effusive volcanic activity of pyroxene and leucocratic andesites in the Javorie and Štiavnica stratavolcanoes continued throughout the Middle-Late Sarmatian age. The volcanic activity was accompanied by asymmetric subsidence in the Upper Nitra, Turiec, Žiar, Bátovce and Zvolen depressions, which were compensated by the accumulation of volcano-sedimantary rocks. **(vi)** The most distinct block movement with vertical displacement up to 3 km took place along N–S and NNE–SSW faults system in the central part of the

region. **(vii)** During the Pannonian to Pontian period the subsidence and limnic sedimentation continued in the Bátovce, Žiar and Turiec grabens.

3. MAGNETIC DATA AND MODELLING

The magnetic map of Slovakia was compiled with a resolution of 250 m flight line spacing (sampling frequency: 1 s) as part of a project titled 'Atlas of Geophysical maps and profiles' (Kubeš et al., 2001). Kubeš et al., (2001) interpreted and modelled all relevant magnetic anomalies. The magnetic map reflects a very complicated geological setting of the Western Carpathians. The values of magnetic anomalies range from 47900 nT to 48600 nT (Magnetic Epoch 1995.5; Rozimant et al., 2009). The source of the anomalies were mainly correlated with the sites of morphological elevations such as mountain ranges of Tertiary and occasionally Quaternary volcanism in the central part of Slovakia (Fig. 2). The neovolcanic mountains dominate the Eastern Slovakian physiography. The Neogene-Quaternary volcanism in the central, southern and eastern Slovakia is a component of an extensive volcanic area situated on the inner part of the Carpathian Arc as a component of the Pannonian Basin (Kubeš et al., 2001). In the magnetic anomaly map, a complex character in the magnetic field can be observed in the central Slovakia. This was also noted in the Eastern Slovakian Lowland (Fig. 2). To remove the distortion of magnetic anomalies caused by the Earth's magnetic field, reduction to pole transformation (RTP) was applied to the magnetic anomalies using the magnetization angle of 65° to the induced magnetization (Fig. 3).

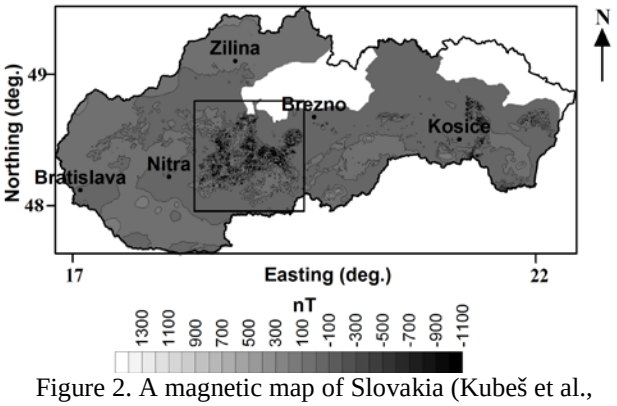

Figure 2. A magnetic map of Slovakia (Kubeš et al., 2001). The square box shows the CSVF. Contour interval = 100 nT.

3.1. Magnetic anomalies of central volcanics

The Magnetic anomalies of CSVF show a very complex pattern (Fig. 2). We decided to investigate the portion of this anomalous region (marked in box in Fig. 2) so as to find the characteristics of the source body. RTP transformation was applied to extract the selected portion of the magnetic map (Fig. 3).

The upward continuation is an analogy to the low-pass filtering technique and can be done by multiplying the Fourier transform of the anomaly by the following equation:

$$\exp\left[-2\pi h\left(k_x^2 + k_y^2\right)^{1/2} / N\right]$$ (Kanasewich & Agarwal, 1970), where h is the continuation distance; k_x and k_y are the wave numbers in the x and y spatial directions; and N is the total number of the data points (grid numbers). The high topographic regions are reflected in the residual magnetic anomalies as high frequencies. Therefore, a 3-km upward continuation was applied to the residual aeromagnetic anomalies in order to remove the effects of topography (Fig. 4). The upward continued magnetic anomalies do not correlate with the topography and they mainly reflect the anomalies of the deep-seated magnetized bodies. Results of the upward continuation show the presence of disoriented anomalies in the deeper section profiles. Normally, surface topographic features may have some effect on the magnetic anomalies. When the magnetic anomalies are disoriented normally, the surface features may affect the magnetic anomalies. Because the surface effects are well suppressed in the 3 km upward continued aeromagnetic map.

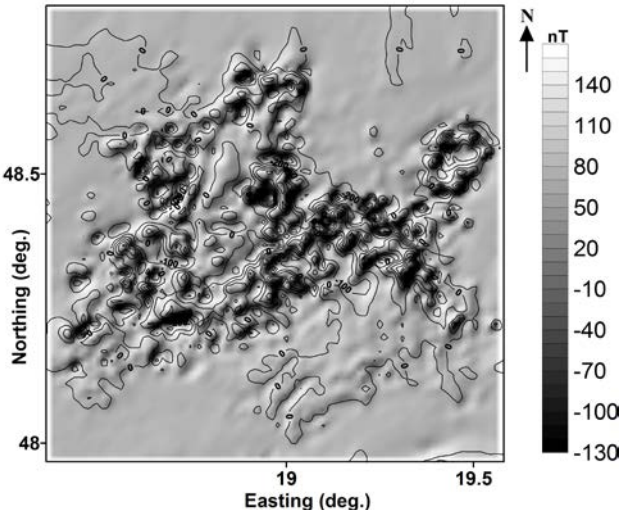

Figure 3. Application of reduction to the pole of the magnetic anomalies of CSVF (Contour interval = 100 nT).

Spector & Grant (1970) gave the relation for the energy spectrum of the model in polar coordinates as follows:

$$r=\left(u^2+\upsilon^2\right) \quad and \quad \theta=\left(\tan^{-1}\left(u/\upsilon\right)\right)$$

$$E\left(r,\theta\right)=\left|F\left(\Delta T\right)\right|$$

$$=4\pi^2k^2e^{-2hr}\left(1-e^{tr}\right)^2S^2\left(r,\theta\right)R_T^2\left(\theta\right)R_k^2\left(\theta\right) \quad (1)$$

where $k/4ab$ is the magnetic moment/ unit volume of the body (k is the magnetic moment/ unit depth),

$$S\left(r,\theta\right)=\frac{\sin\left(ar\cos\theta\right)}{ar\cos\theta}.\frac{\sin\left(br\cos\theta\right)}{br\cos\theta}$$

$$R_T^2\left(\theta\right)=\left[n^2+\left(l\cos\theta+m\sin\theta\right)^2\right],$$

$$R_k^2\left(\theta\right)=\left[N^2+\left(L\cos\theta+M\sin\theta\right)^2\right]$$

l,m,n direction cosines of geomagnetic field.

The azimuthally averaged power spectrum suggested by Spector & Grant (1970) was applied to the 3-km upward continued anomalies and from that we have estimated that the top of the anomaly source is at a depth of 4.4 km (Fig. 5).

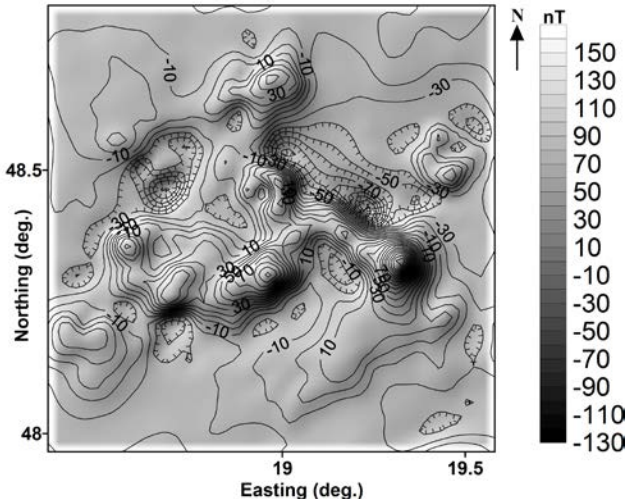

Figure 4. The upward continued (3 km) map of Central Volcanics. Contour interval = 10 nT

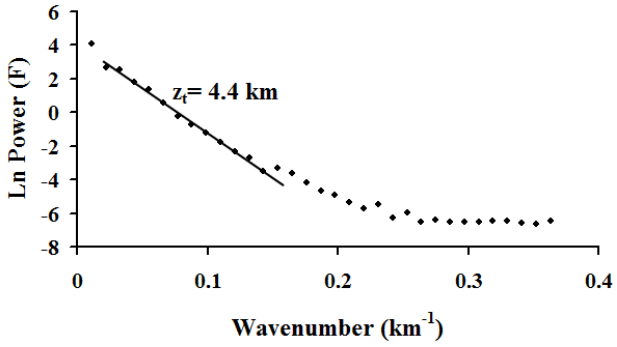

Figure 5. The power spectrum showing wavenumber vs. power (log

3.2 Three-dimensional modelling

An interesting method for modelling the aeromagnetic anomalies was introduced by Kearey (1991). Many applications were realized based on this method (Ates & Kearey, 1993; Ates & Kearey, 1995; Ates et al., 1997; Büyüksaraç et al., 2005) to model aeromagnetic anomalies in Southern England, Western Turkey and the Cappadocia region of Turkey. Based on this method, the pseudogravity anomalies were produced from the 3-km upward continued anomalies using 65° inclination and 3.5° declination angles of the geomagnetic field and body magnetization (Valach et al., 2006). The ratio of the intensity of magnetization to density (J/Δρ= 1 mA m^2/kg) is assumed to be uniform. The pseudogravity anomalies constructed by using these parameters are shown in figure 6.

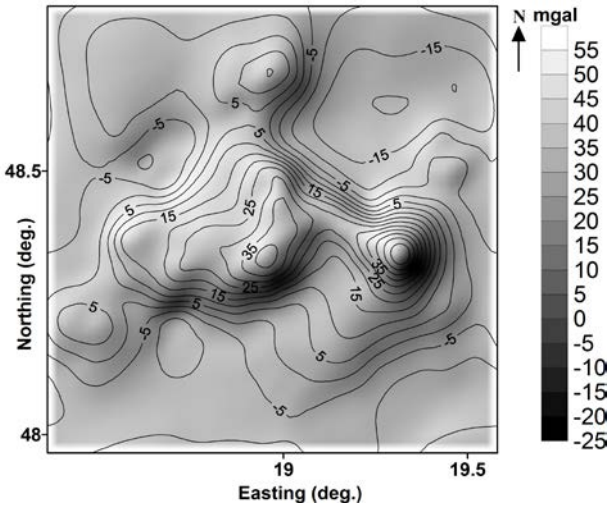

Figure 6. A pseudogravity anomaly map of the CSVF. Contour interval = 5 mGal.

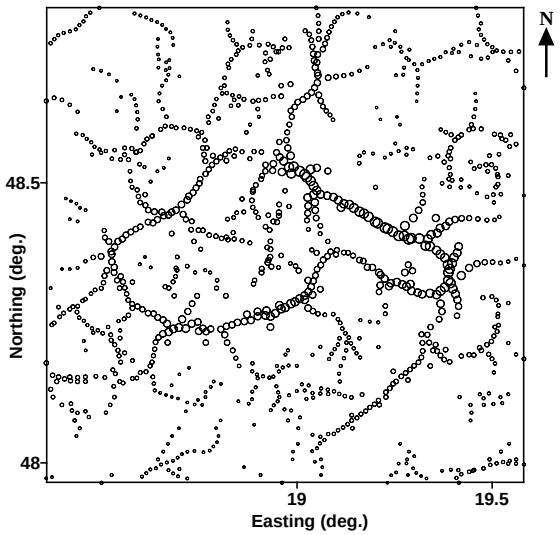

Figure 7. Locations of the maxima of the horizontal gradient of pseudogravity for the CSVF. The size of circles is proportional to the magnitude of the gradient.

The method developed by Blakely & Simpson (1986) that locates the edges of anomalous bodies, has been applied to the anomalies shown in figure 6. The maxima of the horizontal gradients are calculated

from the pseudogravity anomalies. These maxima are displayed as circles, and the size of the circles denote the magnitude of the horizontal gradients. The locations of the maxima of the horizontal gradient map are shown in figure 7.

The pseudogravity anomalies have been projected on a 1.4 × 1.4 km grid scale. The pseudogravity anomalies were modelled using a 3D gravity-modelling program based on the Cordell & Henderson (1968) method. In 3D modeling method of Cordell & Henderson (1968), the gravity anomaly is digitised on a rectangular grid. This method assumes that the causative body can be approximated by means of a bundle of vertical, elemental prisms, each having a cross-sectional area of grid square and a uniform density. Three options are available in this method: the reference plane may optionally be chosen to delimit the base, the top or the midpoint of the prism elements. An initial approximation of structure is calculated by means of the Bouguer slab relationship given in Eq. 2. The ratio of the observed to calculated gravity is used to iterate the first and successive models until a good match is reached (Iteration can be performed from 1 to n^{th} step until a good fit is achieved between the observed and the calculated gravity data where "n" is the iteration number).

$$K = \frac{1}{2\pi\gamma\rho} \qquad (2)$$

$$t_{1,q} = Kg_{obs,q}$$

$t_{1,q}$: Thickness of the prism obtained from the first iteration at the q^{th} grid point
g_{obs}: Observed gravity
γ: International gravity constant
ρ: Density
$t_{n,q}$: Thickness of the prism obtained from the n^{th} iteration at the q^{th} grid point.

The ratio of the observed to the calculated gravity is used to modify the first and successive models until a good fit between them is reached. A flat-bottomed model was first chosen and depth of the base was iteratively adjusted until the top of the model reached to 4.4 km, estimated by power spectrum analysis. By applying this technique, we suggest that in case of CSVF, the base of the model causative body lies at a depth of 8.5 km (Fig. 8).

4. DISCUSSIONS AND CONCLUSIONS

The magnetic map of Slovakia exhibits a complicated anomaly pattern. In the central part, there are stronger magnetic anomalies than elsewhere probably because of presence of intensive magnetized rocks and also because of isostasy. The RTP transformed anomalies clearly reflects the volcanic effects on the map (Fig. 3).

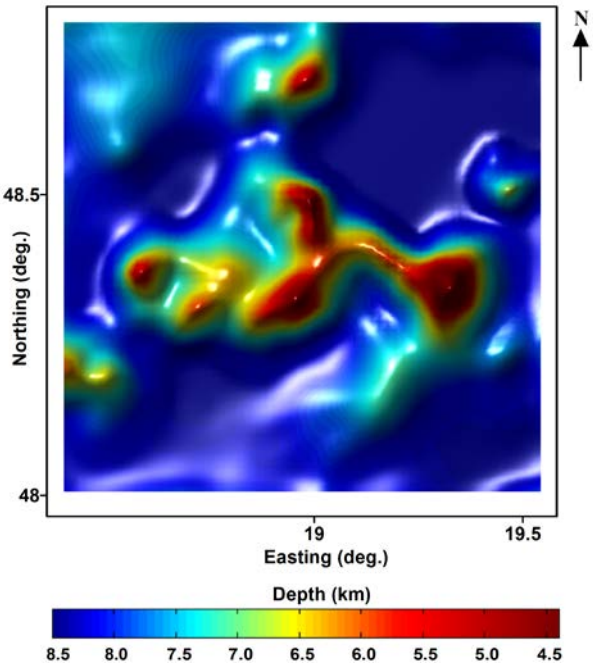

Figure. 8. Three-dimensional model of CSVF.

Upward continual aeromagnetic anomalies (Fig. 4) demonstrate that the deep magnetic body must have a magnetization vector that has a different orientation from that of the present day magnetic field (declination 3.5°, inclination 65°). When the magnetic anomalies are disoriented by the tectonic regime, the disorientation of the magnetic anomalies can be extended down to the bottom of the magnetic crust (Curie point depth).

The azimuthally averaged power spectrum was applied to the 3-km upward continued anomalies in the Central Volcanics, and the source was estimated to be at a depth of 4.4 km (Fig. 5).

The pseudogravity anomalies were modelled using a 3D gravity modelling program based on the Cordell & Henderson (1968) method. From this method, we infer that the bottom of the magnetic body in this region is at a depth of 8.5 km from the surface (Fig. 8), which corresponds to the Curie Point Depth of Slovakia (estimated by Rozimant et al., 2009). This deep-seated magnetized body may be the source for the widespread volcanic activity of the Central volcanics of Slovakia. The shallow Curie Point Depths indicate the high geothermal gradient of the study area.

The maxima of the horizontal gradients are calculated from the pseudogravity anomalies (Fig. 7).

When we correlated the 3D modelling with the maxima of the horizontal gradients, the edge of the body could be bordered by the maximas. Konečný & Lexa (2002) had published a map of CSVF (Fig. 9). Our results are in agreement with Konečný & Lexa (2002). Figure 10 presents the edge of the volcanic complexes and some lineaments. They have been numbered on the correlated map in figure 10.

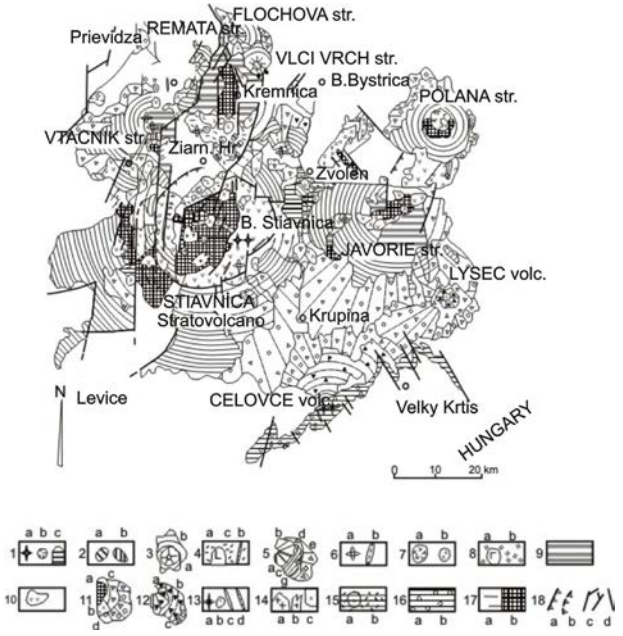

Figure 9. The structural scheme of the Central Slovakian Volcanic Field (after Konečný & Lexa, 2002). *Pannonian to Quaternary*: 1- sediments of intravolcanic depressions; 2- products of the alkali basalt volcanism, a- necks, b- cinder cones and c- lava flows; *Pannonian*: 3-lava flows and sills of aphanitic calc-alkali basalts / basaltic andesites (a) and pyroxene andesites (b); 4- a stratovolcano of porphyritic calc-alkali basalts / basaltic andesites, a- volcanic cone and b- effusive complex; *Middle to Late Sarmatian*: 5- rhyolite domes / dome flows (a), dykes (b) and pyroclastic and epiclastic rocks (c) of the Jastraba formation; *Early to Middle Sarmatian*: 6- andesite stratovolcanoes, a- effusive cones, b- stratovolcanic cones, c- stratovolcanic complex of the proximal zone, d- epiclastic volcanic breccias of the proximal zone, e- epiclastic volcanic breccias and conglomerates of the proximal/distal zone, f- epiclastic volcanic conglomerates and sandstones of the distal zone, g- tuffaceous sediments; 7- andesite necks (a) and dykes (b); 8- andesite extrusive domes (a) and diorite porphyry intrusions (b); 9- rhyodacite domes/dome flows (a) and related pumice tuffs and reworked tuffs (b) of the Strelniky formation; *Late Badenian*: 10- basaltic andesite / andesite effusive complexes with hyaloclastites and phreatomagmatic pyroclastic rocks filling grabens; 11- dome/flow complexes and related breccias of intermediate to acid andesites filling grabens and caldera; *Early to Middle Badenian*: 12- andesite stratovolnanoes: a- propylitized complex of the central zone, b- stratovolcanic complex of the proximal zone, c- epiclastic volcanic breccias of the proximal/distal zone, epiclastic volcanic conglomerates and sandstones of the distal zone; 13- andesite pyroclastic volcanoes, a- pyroclastic cones, pyroclastic complexes of the proximal zone, c- epiclastic volcanic breccias and conglomerates of the proximal/distal zone; 14- andesite necks (a), quartz-diorite porphyry sills (b) and dykes (c), andesite dykes (d); 15- subvolcanic intrusions, a- granodiorite, b- granodiorite porphyry, c- diorite and diorite porphyry; *Early Badenian*: 16- extrusive domes (a) and related breccias (b) of garnet-bearing andesites in the terrestrial environment; 17- andesite extrusive domes (a) and volcanoclastic rocks of the Vinica formation; 18- *pre-volcanic basement*: a- Early Miocene sediments, b- older rocks, 19- *faults*: a- marginal faults of volcanotectonic grabens, b- marginal faults of the caldera, c- marginal faults of volcanotectonic horsts, d- other faults; and 20- state boundary.

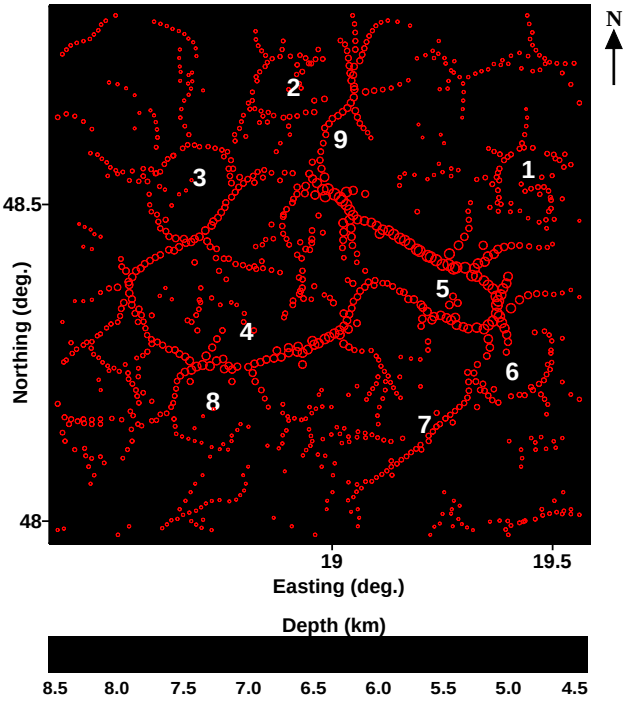

Figure 10. Interpretation of some structural units based on the maxima of the horizontal gradient and 3D model correlated with Konečný & Lexa (2002)'s structural map of CSVF. 1: Pol'ana stratavolcano, 2: Flochova stratavolcano, 3: Vtáčnik stratavolcano, 4 and 5: main Central Slovakia Volcanic Field (CSVF), 6: Lysec stratavolcano, 7 and 9: Lineaments and 8: Štiavnica stratavolcano.

Acknowledgments

We thank the State Geological Institute of Dionýz Štúr for providing us with the aeromagnetic data. Our kindest thanks go to Prof. Dr. M. Bielik, Dr. S.A. Saada and an anonymous reviewer for their comprehensive and delicate review of this paper.

REFERENCES

Ates, A. & Kearey, P., 1993. *Deep structure of the East Mendip Hills from gravity, aeromagnetic and*

seismic reflection data. J. Geol. Soc. London, 150, 1055–1063.

Ates, A. & Kearey, P., 1995. *A new method for determining magnetization direction from gravity and magnetic anomalies: application to the deep structure of the worcester graben*. J. Geol. Soc. London, 152, 561–566.

Ates, A., Sevinc, A., Kadioglu, Y.K & Kearey, P., 1997. *Geophysical investigations into the deep structure of the Aydin - Milas region, Southwest Turkey: Evidence for the possible extension of the Hellenic arc*. Israel Journal Earth Sci., 46, 29-40.

Bielik, M., Sefara, J., Kovac, M., Bezak, V. & Plasienka, D., 2004. *The Western Carpathians - interaction of hercynian and Alpine processes*. Tectonophysics, 393, 63–86.

Bielik, M., Kloska, K., Meurers, B., Svancara, J., Wybraniec, S. & CELEBRATION 2000 Potential Field Working Group, 2006. *Gravity anomaly map of the CELEBRATION 2000 region.* Geologica Carpathica, 57, 145-156.

Blakely, R.J. & Simpson, R.W., 1986. *Approximating edges of source bodies from magnetic or gravity anomalies*. Geophysics, 51, 1494 - 1498.

Büyüksaraç, A., Jordanova, D., Ateş, A. & Karloukovski, V., 2005. *Interpretation of the gravity and magnetic anomalies of the Cappadocia region, Central Turkey*. Pure and Applied Geophysics, 162, 2197-2213.

Cordell, L. & Henderson, R. G., 1968. *Iterative three-dimensional solution of gravity anomaly data using a digital computer*. Geophysics, 33, 596-601.

Kearey, P., 1991. *A possible source of the South-central England magnetic anomaly: basaltic rocks beneath the London Platform*. J. Geol. Soc. London, 148, 775–780.

Kanasewich, E.R. & Agarwal, R.G., 1970. *Analysis of combined gravity and magnetic fields in wave number domain.* J. Geophys. Res., 75, 5702–5712.

Konečný, V. & Lexa, J., 2002. *Evolution of the Central Slovakia Neogene volcanic field related to the horst/graben structure.* Geologia Carpathica, 53, Proceedings of XVII. Congress of Carpathian-Balkan Geological Association Bratislava, September 1st - 4th.

Kubeš, P., Konečný, V., Filo, M. & Simon, L., 2001. *Magnetic anomalies sources of the Tertiary and Quaternary volcanism of the Western Carpathians on the territory of the Slovak Republic*. Mineralia Slovaca, 33, 306.

Plašienka, D., Grecula, P., Putis, M., Kováč, M. & Hovorka, D., 1997. *Evolution and structure of the Western Carpathians: An overview in geological evolution of the Western Carpathians (eds. Grecula, P., Hovorka, D. and Putis, M.)*. Mineralia Slovaca, Bratislava, 1–24.

Rozimant, K., Büyüksaraç, A. & Bektaş, Ö., 2009. *Interpretation of the magnetic anomalies and estimation of depth of magnetic crust in Slovakia*. Pure and Applied Geophysics, 166, 471-484.

Šefara, J., Bielik, M., Konečný, P., Bezák, V. & Hurai, V., 1996. *The latest stage of development of the lithosphere and its interaction with the astenosphere (Western Carpathians).* Geologica Carpathica 47, 6, 339—347

Spector, A. & Grant, F.S., 1970. *Statistical models for interpreting aeromagnetic data*. Geophysics, 35, 293-302.

Túnyi, I. & Márton, E., 2002. *Cenozoic paleomagnetic rotations. In the Inner West Carpathians. Geologia Carpathica*. 53, Proceedings of XVII. Congress of Carpathian-Balkan Geological Association Bratislava, September 1st - 4th.

Valach, F., Váczyová, M. & Dolinsky, 2006. *New Slovak geomagnetic repeat station network*. Earth Planets Space, 58, 751–755.

Zeyen, H., Dérerová, J. & Bielik, M., 2002. *Determination of the continental lithospheric thermal structure in the Western Carpathians: Integrated modelling of surface heat flow, gravity anomalies and topography*. Phys. Earth and Planet. Inter., 134, 89–104.

Received at: 12. 04. 2012
Revised at: 07. 08. 2013
Accepted for publication at: 26. 08. 2013
Published online at: 07. 09. 2013